*Journal of the Geological Society, London*, Vol. **161**, 2004, pp. 983–993. Printed in Great Britain.

# Microbial silicification in Iodine Pool, Waimangu geothermal area, North Island, New Zealand: implications for recognition and identification of ancient silicified microbes

BRIAN JONES[1], KURT O. KONHAUSER[1], ROBIN W. RENAUT[2] & RAYMOND S. WHEELER[1]

[1]*Department of Earth and Atmospheric Sciences, University of Alberta, Edmonton, Alberta, T6G 2E3, Canada (e-mail: Brian.Jones@ualberta.ca)*

[2]*Department of Geological Sciences, University of Saskatchewan, Saskatoon, Saskatchewan, S7N 5E2, Canada*

**Abstract:** Silicified microbes provide evidence for some of the earliest life forms on Earth. They are extremely important to understanding the early development of life and the conditions that allowed its development. Such discussions commonly rely on comparisons with extant taxa and therefore depend upon the preservation style of the microbes and, in particular, the preservation of the taxonomically important features. Silicified microbes are deceptive: they commonly appear to be well preserved even though their taxonomically critical features have been destroyed by silicification. An understanding of the early taphonomic processes that influence microbial silicification can be obtained by studying extant microbes that are being silicified in modern hot spring pools. Iodine Pool, located in the Waimangu geothermal area on the North Island of New Zealand, is ideal for this purpose. The spring water has a temperature of 69–100 °C, a pH of 8.3–9.0, and 440–457 ppm $SiO_2$. Glass slides left in the shallow marginal waters of this pool for 90 h became covered with thin layers of opaline silica, discrete opal-A spheres, unsilicified microbes, pseudofilaments, partly silicified microbes and silicified microbes. The rapidly silicified microbes appear well preserved with their general morphology, diameter, length, and presence or absence of septa being readily apparent. Most of the silicified microbes, however, lack the key features that would allow accurate comparisons with extant taxa. Only two of the silicified microbes can be tentatively allied with the unsilicified forms, despite being found side by side on the same glass slide. These problems in identifying modern, rapidly silicified microbes suggest that identifications of ancient silicified microbes can be problematic and must be treated with caution.

**Keywords:** New Zealand, Waimangu geothermal area, silicification, microbes, hot springs.

Much of our knowledge regarding the origin and development of life on Earth comes from Precambrian silicified microbes found at localities throughout the world (e.g. Walsh & Lowe 1985; Schopf & Packer 1987; Awramik 1992; Walsh 1992; Schopf 1993, 1994; Rasmussen 2000; Westall *et al*. 2001; Schopf *et al*. 2002). Identification of those silicified entities as microbes relied largely on morphological comparisons with extant, unsilicified microbes and, more recently, geochemical signatures (e.g. Buick 1990; Rosing 1999; Shen *et al*. 2001). Some of these identifications have led to the assessment that bacteria (including cyanobacteria) were among the earliest life forms on Earth. Brasier *et al*. (2002), however, questioned the biogenic validity of microfossils from the early Archaean Apex Chert in Australia and suggested that they may be artefacts created by abiogenic processes. Irrespective of this possibility, assignment of any silicified microbe to a particular taxon or group of microbes ultimately depends on the preservation of taxonomically important features, which is largely influenced by early taphonomic processes.

The early taphonomic processes that control microbe silicification can be assessed by experimental silicification of microbes (e.g. Oehler & Schopf 1971; Oehler 1976; Francis *et al*. 1978; Ferris *et al*. 1988; Birnbaum *et al*. 1989; Westall *et al*. 1995; Westall 1997; Toporski *et al*. 2002) or by examining naturally silicified microbes (e.g. Schultze-Lam *et al*. 1995; Jones *et al*. 2001; Mountain *et al*. 2003; Smith *et al*. 2003). This research has, for example, indicated that silicification must take place rapidly for the microbe morphology to be preserved and certainly before the microbes have started to decay (e.g. Bartley 1996; Jones *et al*. 2001). Nevertheless, comparison of the information obtained by these different approaches commonly yields incompatible results and conclusions.

This study is based on a simple experiment whereby small glass slides were placed in Iodine Pool, which is located in the Waimangu geothermal area on the North Island of New Zealand (Figs 1 and 2). This pool was chosen because its waters, which are supersaturated with respect to amorphous silica (opal-A), are ideal for rapid microbial silicification. The glass slides, which were left in the pool for *c*. 90 h, became covered with opal-A precipitates and dense arrays of microbes that have been silicified to varying degrees (Fig. 3). This study (1) compares the salient physical features of the unsilicified and silicified microbes, (2) assesses the stages of very early silicification that are involved in preservation of the microbes, and (3) determines if all the silicified filamentous structures observed were truly microbes. Integration of this information provides important insights into the preservation potential of the microbes and hence, their taxonomic fidelity.

## Setting

The Waimangu–Rotomahana hydrothermal system lies along the southern edge of the Okataina Volcanic Centre in a region of Quaternary rhyolitic ignimbrites and lavas. Iodine Pool, located in Lower Haumi Valley, is one of several geothermal features that formed after the eruption of Mt. Tarawera volcano in 1886

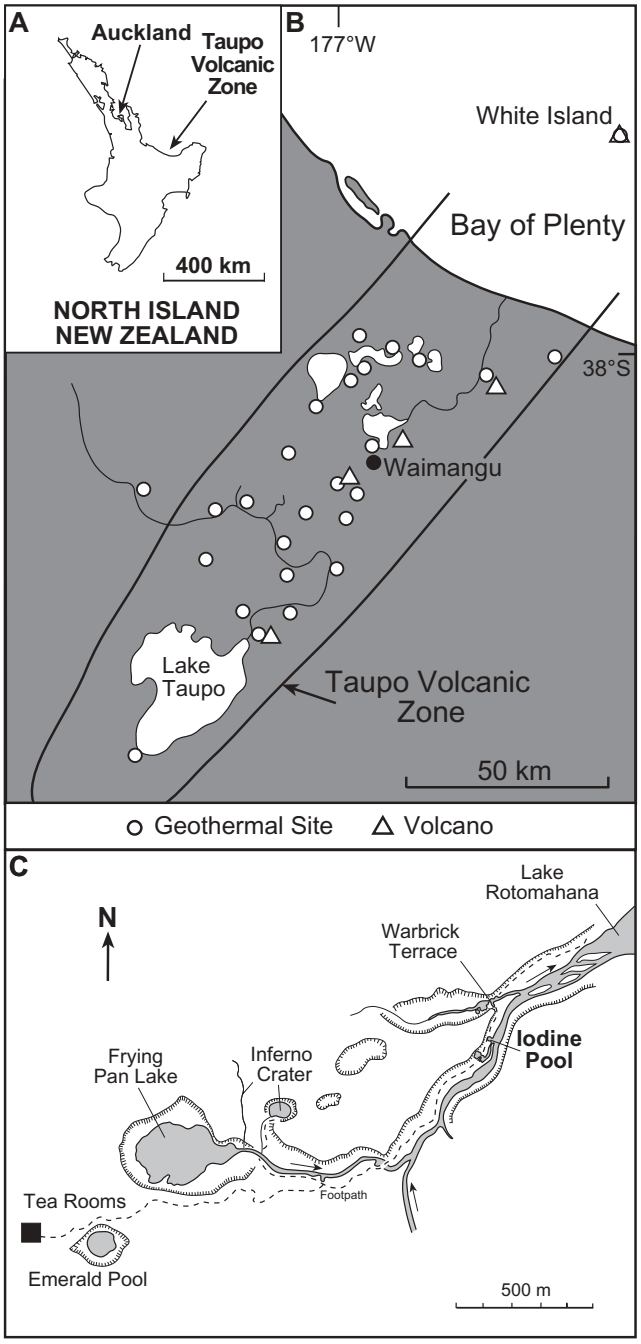


**Fig. 1.** Map showing location of the Waimangu geothermal area in the Taupo Volcanic Zone on the North Island of New Zealand.

(Seward & Sheppard 1986). Iodine Pool, which is *c*. 7 m in diameter and up to 2 m deep, contains water that comes from a perennial spring that is located about 0.5 m above water level on the north side of the pool (Fig. 2a). At times, the spring flows continuously; at other times it acts as a small geyser issuing a jet up to 70 cm in the air. The outflow water discharges through an artificial drain (below a road) onto Marble Terrace, a broad sinter apron that is covered by microbial mats.

The spring above the pool, which ejects water with an average temperature of 97 °C, is one of the hottest springs in the area (Scott 1992). The chloride–bicarbonate–sulphate water in Iodine Pool has a pH of 9.0, up to 470 mg $l^{-1}$ $SiO_2$, and a temperature of 69–81 °C, with the cooler water being in the shallow marginal areas (Table 1) (Sheppard 1986; Simmons *et al*. 1994). Unlike many hot spring pools in the Taupo Volcanic Zone, the water in Iodine Pool is supersaturated with respect to opal-A, which precipitates rapidly without significant cooling or evaporation. Precipitates of opal-A cover all submerged substrates, including tree branches (Fig. 2b) and leaves derived from the steep wooded slopes west of the pool. Most of the sinter is pale greyish brown and granular in appearance, but is none the less commonly hard and well cemented. Green, orange and yellow bacterial mats up to 30 cm wide line the gently sloping subaerial margins of the pool, but are absent below water level.

## Materials and methods

New glass slides (7.5 cm × 5.0 cm and 7.5 cm × 2.5 cm) were placed in the shallow water along the edge of Iodine Pool (Fig. 2) for a period of *c*. 90 h in February 2003. Some slides were laid flat on the substrate, completely immersed in water up to 20 cm deep, whereas others were placed vertically, either embedded in siliceous sediment or resting against sinter-coated rocks. Upon retrieval, the slides, which were visibly coated in silica and pale brown films, were placed in plastic vials and transported to the laboratory. There, the slides were mounted on SEM stubs and sputter coated with a very thin layer of gold or chrome and then examined on a JEOL 6301F field emission scanning electron microscope (FE-SEM) at an accelerating voltage of 2.5–5 kV. Obtaining high-magnification, high-resolution images of the collapsed unsilicified microbes was difficult because they lacked relief, and the instability of gold coatings on these filaments caused micro-desiccation cracks and migration of the gold. Coating these microbes with chrome produced better images.

This study is based largely on 542 scanning electron micrographs of the microbes and precipitates found on the glass slides that had been placed in Iodine Pool. Dimensions of the unsilicified and silicified microbes were determined from these images. Water temperature and pH were measured in the field. Non-acidified water samples were filtered to 0.45 μm in the field and subsequently to 0.2 μm in the laboratory prior to analysis. Water samples were analysed, within 1 month of collection, by atomic absorption spectrometry (Na, K, Ca, Mg, Si), ion chromatography ($SO_4$), ion-specific electrodes (Cl, F, Li), and titration ($HCO_3$, $CO_3$).

## Microbes

The microbiota consists of a diverse assortment of unsilicified microbes (Figs 4 and 5), partly silicified microbes (Fig. 6), pseudofilaments (Fig. 7) and silicified microbes (Figs 3 and 8). From their state of preservation, abundance and monospecificity in some samples, the thermophilic bacteria and Archaea that coat the slides are believed to represent organisms that were living in the pool. It is possible, however, that some of the microbiota could have been blown or washed in from the pool margins (e.g. on plant debris). The fact that these microbes colonized the glass slides while they were submerged in the pool is shown by microbes that rest on top of precipitated layers and spheres of opal-A, and unsilicified microbes that are commonly wrapped around the silicified microbes (Fig. 3b). The absence of microbes or precipitates on new glass slides that had not been placed in the water shows that microbes had not colonized the slides before being placed in the pool. Some slides contained silicified spores and abraded diatom frustules that must have been blown or washed into the pool.

### *Unsilicified microbes*

Unsilicified microbes lie on top of silicified filaments and layers of opal-A precipitates that coat the glass slides (Fig. 4). These

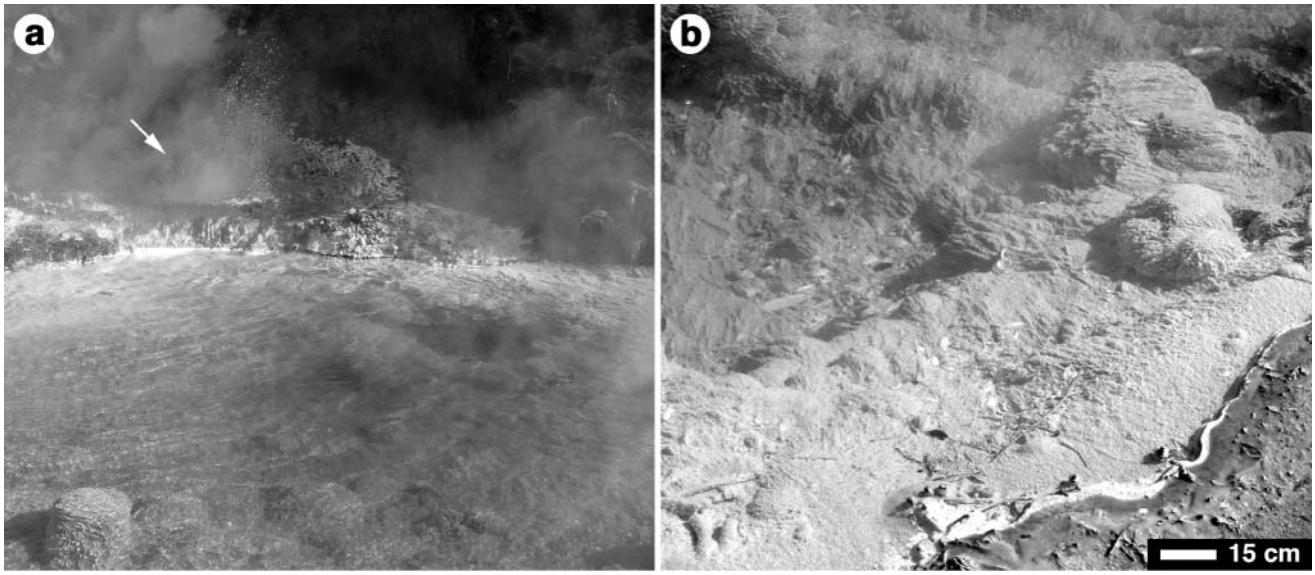


**Fig. 2.** Iodine Pool, Waimangu. (**a**) General view of Iodine Pool with spring in background (arrow). (**b**) Marginal area of pool where glass slides were placed. Note silica precipitates covering floor of pool. Photograph taken in 2000; branches have since been removed from pool.

**Table 1.** *Composition of spring water in Iodine Pool, Waimangu Geothermal Valley*

| No. | Date | *T* (°C) | pH | Li | Na | K | Mg | Ca | $SiO_2$ | B | F | Cl | $SO_4$ | $HCO_3$ |
|---|---|---|---|---|---|---|---|---|---|---|---|---|---|---|
| 1 | May 1977 | 99.0 | 7.7 | 4.0 | 529 | 68.0 | 0.16 | 4.87 | 427 | 8.00 | 3.3 | 712 | 107 | 180 |
| 2 | April 1982 | 81.0 | 9.0 | 4.0 | 550 | 62.0 | 0.02 | 3.31 | 447 | 6.71 | 3.9 | 745 | 112 | 241 |
| 3 | April 1982 | 99.0 | 7.6 | 3.7 | 520 | 59.0 | 0.02 | 3.31 | 470 | 3.53 | 3.9 | 720 | 101 | 563 |
| 4 | April 1982 | 100.0 | 9.3 | 2.2 | 350 | 44.0 | 0.01 | 2.86 | 297 | 3.51 | 1.3 | 442 | 108 | 140 |
| 5 | April 2000 | 82.0 | 8.9 | 3.6 | 547 | 64.5 | 0.15 | 4.15 | 445 | 5.60 | 3.6 | 734 | 110 | 210 |
| 6 | Feb. 2003 | 69.1 | 8.2 | 3.6 | 540 | 66.0 | 0.04 | 3.50 | 457 | 4.80 | 4.0 | 728 | 108 | 240 |
| 7 | Feb. 2003 | 69.0 | 8.3 | 3.6 | 555 | 68.0 | 0.02 | 3.40 | 440 | 4.72 | 4.0 | 740 | 108 | 255 |

1. Iodine Pool, Giggenbach (1995)
2. Iodine Pool, Seward & Sheppard (1986, table 7.1), in mg/kg.
3. Geyser above Iodine Pool, Seward & Shepherd (1986, table 7.1), in mg/kg.
4. Spring below road, Seward & Sheppard (1986, table 7.1), in mg/kg.
5. Iodine Pool, this study.
6. Iodine Pool, this study.
7. Outflow channel, opposite side of road from Iodine Pool.

filaments, which are flattened because of collapse of the soft tissues, are wider than the diameter of the original tube-shaped filament (Fig. 4a). Where an individual filament changes from its 3D form to a flattened form, the flattened form is about twice the width of the original filament (Fig. 4a). Original filament diameters are therefore equated to *c*. 50% of the flattened width. Despite flattening, the filaments display remarkable consistency in their overall dimensions and morphology (Fig. 4).

The microbes are found as discrete entities (Fig. 4a, d and e), epiphytes (Fig. 4b and c), entangled masses with more than one type of microbe (Fig. 4g), or in loose meshworks (Fig. 4h). Contrasting morphology, which is readily apparent in these close associations, attests to the diverse nature of the microbiota (Fig. 4b, c, g and h). For convenience of reference, these collapsed microbes are labelled here as morphotypes CM-A to CM-F.

The unsilicified biota is dominated by CM-A, a septate filamentous microbe that is >500 μm long and, in its flattened form, 0.7–1.0 μm wide (Fig. 4a–c, g and h). The original filament was probably 350–500 nm in diameter. The positions of the septa are indicated by well-defined constrictions in the filament (Fig. 4a–c). There is no evidence of a sheath. Cell length is variable along individual filaments and between filaments (Fig. 5). In some filaments, for example, cell length ranges from 2 to 5 μm. The variable cell length may represent either cells that are dividing into two cells or cells that include intermediate septa that are not evident because of poor preservation. The former notion is supported by the fact that many of the longer cells are about twice the length of the shorter cells (Fig. 5).

CM-B, which is relatively rare, is >500 μm long, *c*. 1.6 μm wide in its flattened form, and characterized by cells that are typically *c*. 3 μm long and 1 μm wide (Fig. 4d). Unlike CM-A, this microbe appears to have been encased by a thin sheath.

CM-C is a filamentous microbe, >500 μm long, with a flattened width of *c*. 400 nm, and a thin sheath (Fig. 4e). Although most appear to be non-septate, others have clearly defined septa (Fig. 4f).

CM-D, a rod-shaped epiphyte, is up to 8 μm long with a flattened width of 300–400 nm (Fig. 4b and c). Although typically found attached to CM-A, there are also scattered, isolated specimens of CM-D that may have been dislodged from the substrate on which they grew (Fig. 4i and j). The significance of the variation in the length/width ratio of these microbes is unknown.

CM-E, which is relatively rare, is a bicellular microbe that is

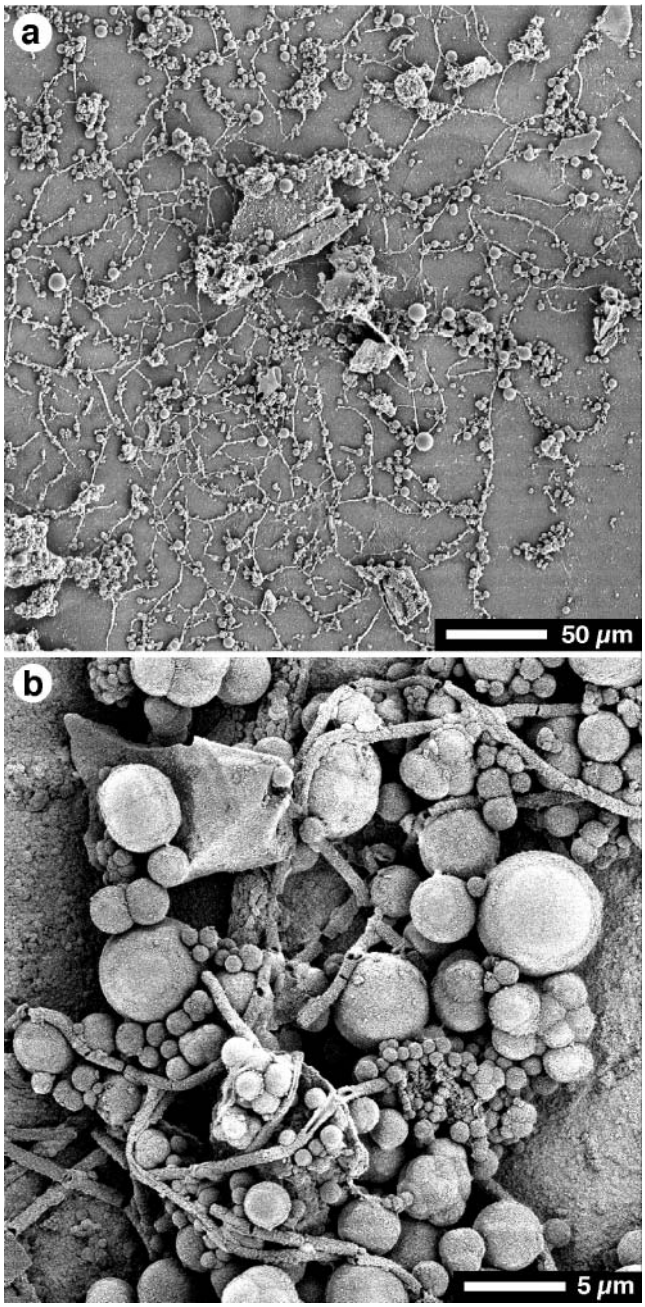


**Fig. 3.** Scanning electron micrographs of colonies of silicified microbes and opal-A precipitates found on glass slides left in Iodine Pool for *c*. 90 h. (**a**) Complex network of silicified microbes associated with opal-A spheres and larger silica fragments that may be detrital in origin. (**b**) Septate filament associated with silica spheres.

up to 4 μm long with a flattened width of *c*. 700 nm (Fig. 4k). It is found as an epiphyte on CM-A (Fig. 4b) or as isolated specimens (Fig. 4k) that may have been dislodged from the substrate that it originally colonized. CM-F, which is up to 2 μm long and *c*. 1 μm in diameter, is probably a sheathed bacterium (Fig. 4l).

### *Partly silicified microbes*

Partly silicified filamentous microbes (mostly CM-A and CM-D) are scattered among unsilicified and silicified microbes (Fig. 6). In some specimens, silicification is evident as irregular-shaped masses of opal-A, <500 nm in diameter, which are located along the axial region of the microbe (Fig. 6a). In other specimens, silicification is more extensive with the opal-A spheres merged in elongate masses that are up to 4 μm long (Fig. 6b and c). The silicified parts, typically restricted to a single cell in a septate filamentous microbe, are consistently located along the axial regions of the microbes.

The silicified axial regions are flanked by collapsed, unsilicified material that may represent a thin sheath that once surrounded the trichome (Fig. 6a–c). The silicified segments can be traced laterally into unsilicified parts that show little or no evidence of silicification (Fig. 6b and c). These specimens are important because they highlight the morphological inconsistency between silicified and unsilicified segments (Fig. 6c). Importantly, in the absence of collapsed non-silicified microbial segments, it would be virtually impossible to attribute the silicified parts to a particular microbe. It would, for example, be impossible to attribute the small oval or elongate masses of opal-A shown in Figure 6a–c to a filamentous microbe if the soft, collapsed parts of the microbe were absent.

### *Pseudofilaments*

Pseudofilaments, which are >500 μm long and 400 nm in diameter, are formed of merged opal-A spheres (Fig. 7a). These structures are morphologically similar in appearance to many of the silicified filamentous microbes (Figs 3 and 8). Traced laterally, however, the silicified 'filaments' pass into 'strings of beads' solely formed of opal-A spheres (300–400 nm diameter), centred around a mucus strand that is <10 nm thick (Fig. 7b and c). The location of the opal-A spheres around the mucus strand and the paucity of spheres in the areas around the structures indicate preferential precipitation around the mucus strand.

### *Silicified microbes*

Silicified microbes are present in complex colonies (Fig. 3) or as individual specimens (Fig. 8). Most features in these microbes are hidden under the opal-A that has encrusted and/or replaced them. The exterior surfaces of the microbes are covered with

**Fig. 4.** Scanning electron micrographs of unsilicified, collapsed filaments on glass slides left in Iodine Pool for *c*. 90 h. (**a**) Unsilicified filament (CM-A) draped over opal-A spheres (white arrow) passing into flattened filament on opal-A precipitates on glass slide. Width of flattened filament is about twice that of the filament. Constrictions mark location of septa (arrows). (**b**) Septate filament (CM-A) with small-diameter, rod-shaped (CM-D) and small bacteriform (CM-E) epiphytes. (**c**) Septate filament (CM-A) with rod-shaped epiphytes (CM-D). (**d**) Large-diameter filament (CM-B) with well-defined septa (arrows) encased by sheath (S). (**e**) Small-diameter filament (CM-C) encased by sheath (S). (**f**) Small-diameter septate filament (CM-C) with well-defined septa (arrows) encased by sheath (S). (**g**) Interwoven septate filaments CM-A and CM-C. (**h**) Two filaments (CM-A) of approximately the same diameter but with cells of different lengths as shown by spacing between arrows. (Note rod-shaped epiphytes (CM-D).) (**i**) Small-diameter, rod-shaped microbe (CM-D). (**j**) Rod-shaped microbe (CM-D). (**k**) Bicellular, rod-shaped microbe (CM-E). (**l**) Bacteriform microbe (CM-F).

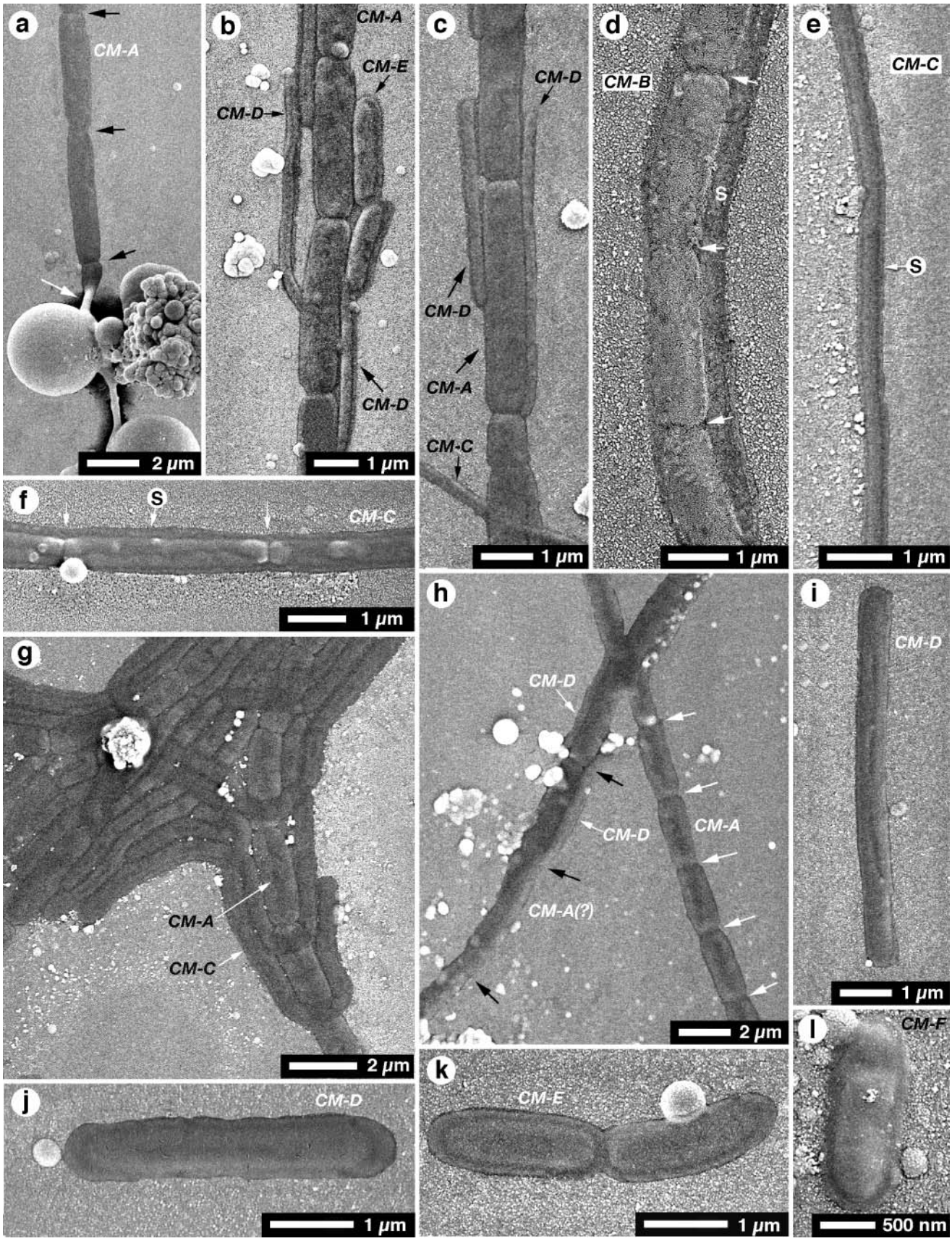
a
CM-A
2 μm
b
CM-A
CM-E
CM-D
CM-D
1 μm
c
CM-D
CM-D
CM-A
CM-C
1 μm
d
CM-B
S
1 μm
e
CM-C
S
1 μm
f
S
CM-C
1 μm
g
CM-A
CM-C
2 μm
h
CM-D
CM-D
CM-A
CM-A(?)
2 μm
i
CM-D
1 μm
j
CM-D
1 μm
k
CM-E
1 μm
l
CM-F
500 nm

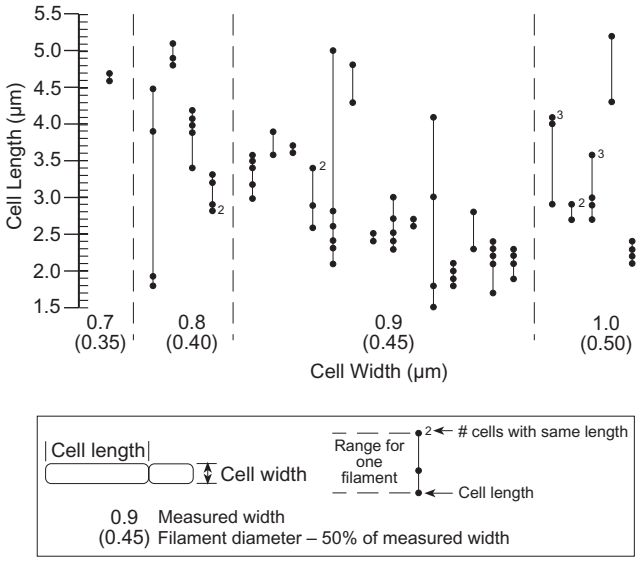


**Fig. 5.** Cell length and width (50% of flattened width) for collapsed, unsilicified septate filaments found on glass slides left in Iodine Pool for *c*. 90 h. Variance in length of cells for single filaments and between filaments should be noted.

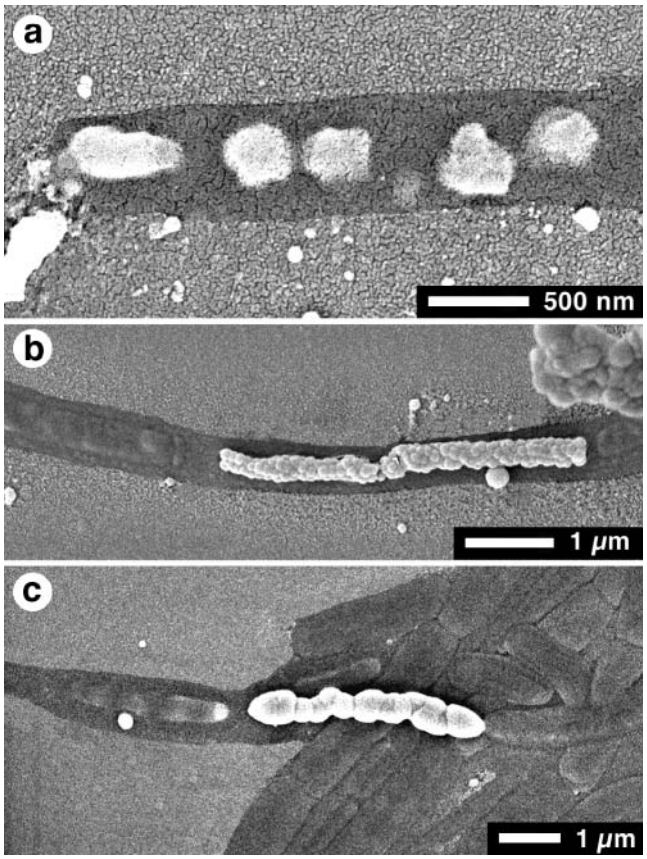


**Fig. 6.** Scanning electron micrographs of partly silicified microbes found on glass slides left in Iodine Pool for *c*. 90 h. (**a**) Small, irregular-shaped masses of opal-A located along axial region of filamentous microbe. (**b**, **c**) Rod-shaped silicified masses located along axial region of collapsed filamentous microbes. Difference in morphology of opal-A spheres and lack of opal-A spheres on surrounding surface should be noted.

small opal-A spheres, large opal-A spheres or smooth opal-A (Fig. 8). Some microbes are entirely covered in multiple layers of opal-A, with each layer being characterized by different styles of precipitates (Fig. 9).

*Small-diameter opal-A spheres.* The diameter of these opal-A spheres, which range from 10 to 300 nm, are typically less than the diameter of the microbe (Fig. 8a-c, e-l). On some specimens, neighbouring opal-A spheres, all of approximately the same size, do not merge and seem to be aligned in distinct rows (Fig. 8g). In other specimens, the opal-A spheres are more variable in diameter, they commonly merge with each other, and they have a random distribution (Fig. 8i). The surface topography of the silicified microbe is controlled by the size and distribution of the opal-A spheres.

*Large-diameter opal-A spheres.* The diameter of these opal-A spheres is greater than the diameter of the microbe (e.g. Fig, 8d, j, m and n). Neighbouring spheres are typically merged so that the microbes appear to be encased in bands of opal-A that are subequal (Fig. 8d and j) or unequal in width (Fig. 8m and n). It is unclear if the constrictions in width between neighbouring bands reflect the patterns of opal-A precipitation or an original morphological feature of the microbe, such as the location of septa (Fig. 8d and e).

*Smooth opal-A surfaces.* Scattered microbes are encased with opal-A that has a smooth surface and appears structureless (Fig. 8q).

*Multiple layers of opal-A spheres.* On some microbes, large opal-A spheres are scattered across layers formed of small opal-A spheres or structureless opal-A (Fig. 8h and q). On other microbes, two layers of encrusting opal-A, characterized by different styles of precipitates and (or) opal-A spheres of difference sizes, are evident (Figs 8r and 9). In these specimens, an inner layer is formed of small (up to 125 nm) opal-A spheres that are arranged in distinct rows (Fig. 9). That layer is encased by a second layer formed of opal-A spheres that are up to 250 nm in diameter, which merge with each other, and seem to be irregularly distributed (Fig. 9b and c). In some specimens, isolated large (up to 750 nm) opal-A spheres rest upon the second layer (Fig. 9b).

## Discussion

Of necessity, experimental silicification of microbes has involved specific taxa and precisely defined experimental conditions (Oehler & Schopf 1971; Oehler 1976; Francis *et al*. 1978; Westall *et al*. 1995; Westall 1997; Fein *et al*. 2002; Toporski *et al*. 2002; Yee *et al*. 2003). Some experiments have involved high-temperature and high-pressure conditions (e.g. Oehler & Schopf 1971; Oehler 1976), whereas in other experiments microbes were submerged in low-temperature, silica-rich waters for periods of up to 6 months (e.g. Francis *et al*. 1978; Westall *et al*. 1995; Toporski *et al*. 2002). These experiments have produced inconsistent results. Some have shown that silicification changes the microbes by causing fragmentation (Oehler & Schopf 1971), increasing coalescence of the filaments, loss of the textures in the sheaths despite the retention of some layering (Oehler 1976), contraction of the cytoplasm, changes in the size and shape of the microbe, extraction of pigment, loss of cross-walls in

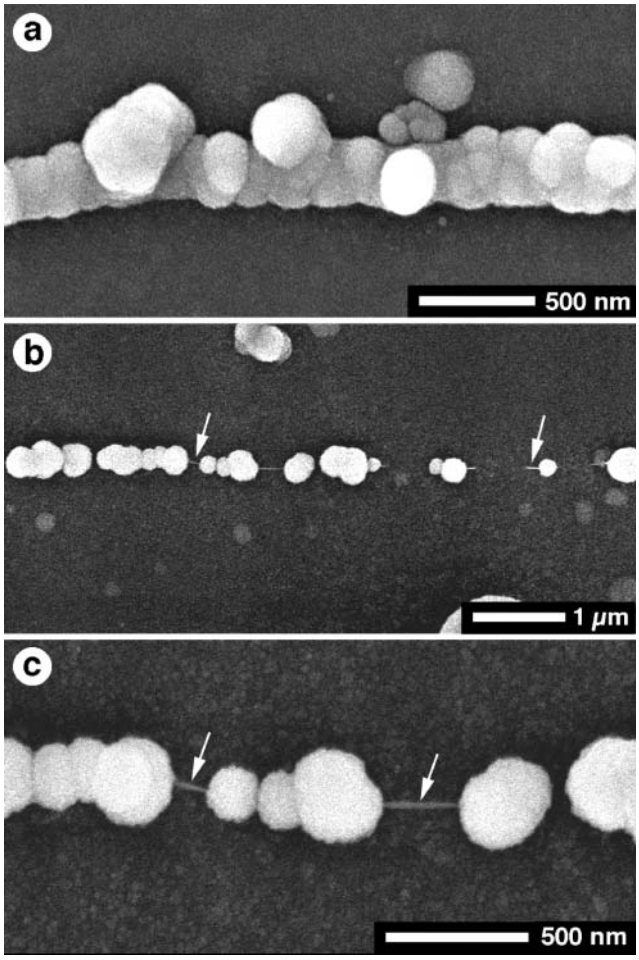


**Fig. 7.** Scanning electron micrographs of pseudofilaments found on glass slides left in Iodine Pool for *c*. 90 h. (**a**) Small-diameter, filament-like structure. (**b**) Lateral continuation of filament-like structure shown in (**a**). Widely spaced opal-A spheres connected by thin mucal strand (arrows) should be noted. (**c**) Opal-A spheres connected by mucal strand (arrows). Similarity between diameters of these opal-A spheres and filament-like structure in (**a**) should be noted.

filamentous microbes, cellular disaggregation (Francis *et al*. 1978), loss of internal cellular details, and decreased preservation of cell-wall details (Toporski *et al*. 2002). Other experiments have shown that some microbes are more prone to silicification than others (Francis *et al*. 1978, table 2; Westall *et al*. 1995; Toporski *et al*. 2002).

The rapidity of opal-A precipitation and microbe silicification in Iodine Pool at Waimangu is not unique. Similar rates of opal-A precipitation were determined for a spring outflow channel at Krisuvik, Iceland (Konhauser *et al*. 2001), and even higher rates were recorded in experiments at other New Zealand hot springs and in the outflow drains of Wairakei geothermal power plant (Mountain *et al*. 2002, 2003; Smith *et al*. 2003). It might be expected that such rapid silicification would produce superbly preserved microbes that display most of their taxonomically important features. For Iodine Pool, it seems reasonable to expect that the silicified microbes could be matched with the unsilicified microbes adhering to the same glass slides. Such comparisons should be possible solely on the basis of morphological criteria and need not involve taxonomic identifications or genetic signatures. In part, this parallels the comparisons that would be made between silicified Precambrian microbes and extant microbes because DNA is not preserved in Precambrian samples.

Partly silicified microbes can be matched with the unsilicified microbes if they are conjoined (Fig. 6). The silicified segments of these microbes, however, are nondescript and apart from their diameter, display no features of taxonomic value. If the silicified segments evident in Figure 6 were not conjoined with the unsilicified collapsed filaments, it would be difficult to relate one to the other. Indeed, it is doubtful that some of the silicified segments would be considered of microbial origin (Fig. 6a). In other cases (Fig. 6b and c), the silicified segments would probably be identified as bacteriform or rod-shaped microbes, not a filamentous microbe. Crucially, many of the pseudofilaments would be considered microbial in origin, leading to questions over the true microbial origins of some Precambrian 'microfossils'.

Morphological information evident from the well-preserved silicified microbes shown in Figure 8 is limited to filament length/diameter and the presence or absence of septa. The unsilicified microbes have a diameter of $<$900 nm with distinct modes at 200–300 nm and 400–500 nm (Fig. 10a). The suggestion that those modes represent different taxa is supported by visual comparisons of the microbes (Fig. 3). The silicified microbes have external diameters that range from 0.3 to 2.9 μm. These diameters are significantly larger than those for the unsilicified microbes (Fig. 10b) and clearly reflect variations in the thickness of the encrusting opal-A. This includes a well-defined mode at 0.5–0.6 μm and a second, weaker mode at 1.0–1.1 μm (Fig. 10b) that may correspond to the two modes evident in the unsilicified microbes (Fig. 10a). Nevertheless, it is difficult to correlate the diameters of the silicified microbes with the diameters of the unsilicified microbes.

Morphologically, it is difficult to relate the silicified microbes to the unsilicified or partly silicified microbes. Based on similarities in size and the presence of septa, the silicified microbe shown in Figure 8a–c may be the same as CM-A (Fig. 4) and the rod-shaped microbe in Figure 8q may be the same as CM-D (Fig. 4i). Other silicified microbes shown in Figure 8, however, cannot be correlated with the unsilicified microbes shown in Figure 3, or the partly silicified microbes shown in Figure 6, with any degree of certainty. Moreover, even if molecular data were available to help identify the dominant taxa in Iodine Pool, the lack of correlation between unsilicified and silicified cells means that the silicified structures would still remain undetermined. The taxonomic fidelity of silicified microbes will depend on the rate of silicification and the factors that control that process. Much of the early research suggested that microbes play an entirely passive role in silica precipitation (e.g. White *et al*. 1956; Walter 1976). Later experimental studies suggested that microbes might act as favourable templates for heterogeneous silica precipitation, through hydrogen bonding or sorption of negatively charged silica ions on positively charged functional groups (e.g. Krumbein & Werner 1983; Ferris *et al*. 1986; Ferris 1993; Schultze-Lam *et al*. 1993, 1995; Konhauser & Ferris 1996). A few studies (e.g. Birnbaum *et al*. 1989) proposed that some bacteria actively concentrate silica in their organic tissues, and it has been demonstrated that bacteria can enhance silica precipitation kinetics in acidic fluids (Fortin & Beveridge 1997). Many recent experimental studies, however, using a variety of conditions and levels of silica saturation, have shown that bacteria generally have a negligible effect on silica nucleation in neutral and alkaline fluids unless the silica is adsorbed onto Fe and Al oxides that are electrostatically bound to the

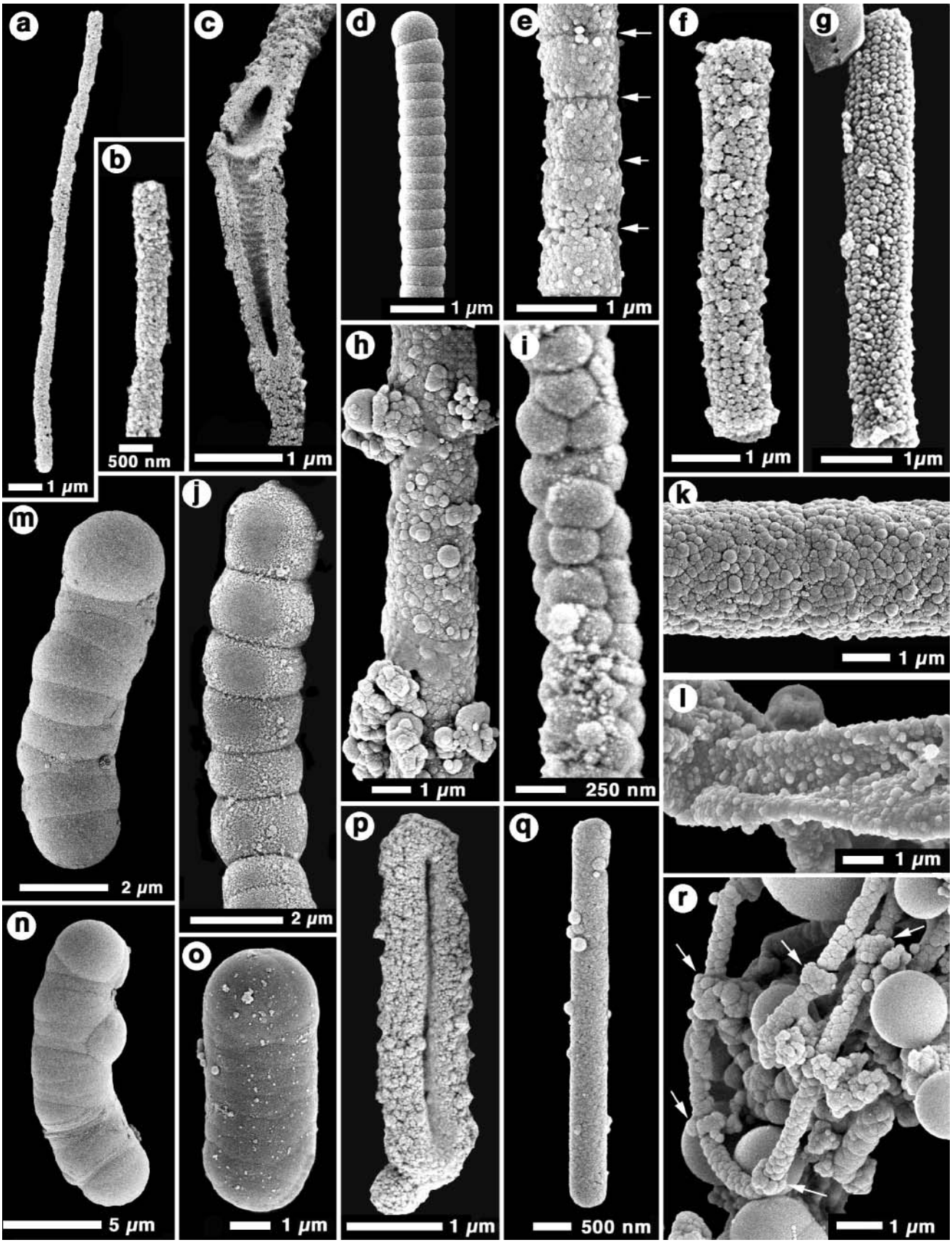
a
1 μm
b
500 nm
c
1 μm
d
1 μm
e
1 μm
f
1 μm
g
1μm
h
1 μm
i
250 nm
j
2 μm
k
1 μm
l
1 μm
m
2 μm
n
5 μm
o
1 μm
p
1 μm
q
500 nm
r
1 μm

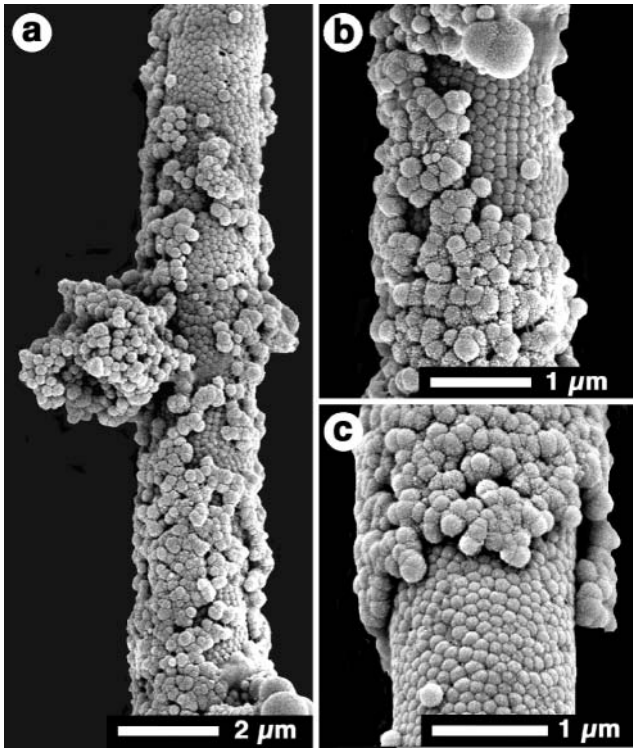


**Fig. 9.** Scanning electron micrographs of filament covered with multiple layers of opal-A spheres, found on glass slides left in Iodine Pool for *c*. 90 h. (**a**) General view of silicified microbe. (**b**, **c**) Multiple layers of opal-A spheres encrusting filament. Contrast in size, shape and organization of spheres in the two opal-A layers should be noted.

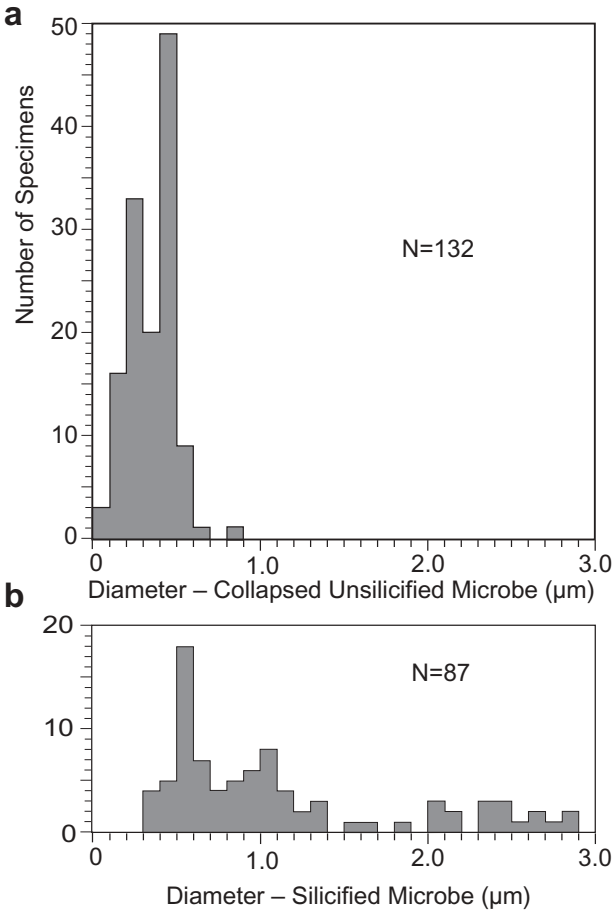


**Fig. 10.** Comparison of diameters of collapsed unsilicified (**a**) and silicified microbes (**b**) found on glass slides left in Iodine Pool for *c*. 90 h. All microbes included irrespective of taxonomy.

bacterial surfaces (e.g. Konhauser *et al*. 1993; Fein *et al*. 2002; Phoenix *et al*. 2003; Yee *et al*. 2003). If passive, the replacement and/or encrustation of the microbes by opal-A should be governed solely by the physicochemical conditions and charge characteristics of cell surfaces. All of the microbes, therefore, should be replaced and/or encrusted with morphologically similar opal-A spheres.

In carbonate systems, microbes that are adorned by different types of calcite crystals gave rise to the suggestion that the calcification style can be taxon specific (e.g. Riding 1991; Merz 1992). By analogy, it could be argued that microbe-specific processes or properties are also responsible for the morphological variations in the opal-A that replaces and encrusts the microbes from Iodine Pool. In most cases, using natural assemblages of silicified microbes to assess any role that microbes played in silica precipitation is difficult because it is impossible to determine if they were all silicified at the same time and hence, under identical physicochemical conditions. However, for the rapidly silicified microbes found on the glass slides in Iodine Pool, the element of time becomes less important, especially given the long-term physical and chemical stability of the spring water (Table 1). A comparison between the silicified microbes found on the glass slides from Iodine Pool reveals the following important points.

(1) The diameter of the opal-A spheres tends to be consistent on individual microbes but variable between microbes. Thus, some microbes are encrusted with opal-A spheres that are significantly smaller than the diameter of the host microbe (Fig. 8e–i), whereas others are encrusted with opal-A spheres that are larger than the diameter of the host microbe (Fig. 8d, j, m and n).

(2) Some microbes are encrusted with opal-A spheres that are regularly arranged (Fig. 8d, e, g, j, m and n), whereas other microbes are encrusted with opal-A spheres that lack any regular distribution pattern (Fig. 8h and i).

(3) More than one layer of opal-A spheres encrusts some microbes (Figs 8h and 9), with successive layers being formed of opal-A spheres that are of different sizes and exhibit different distribution patterns (Fig. 9b and c).

**Fig. 8.** Scanning electron micrographs of silicified microbes found on glass slides left in Iodine Pool for *c*. 90 h (February 2003). (**a**) Elongate septate filament. (**b**) Enlarged view of upper part of filament from (**a**) showing rounded terminus and constrictions indicative of septa. (**c**) Oblique cross-section through elongate filament showing open lumen. From Figure 3b. (**d**) Filament encased with bands of opal-A. (**e**) Filament covered with small opal-A spheres showing constrictions that may denote positions of septa (arrows). (**f**, **g**) Rod-shaped filaments covered with small opal-A spheres. (**h**) Filament covered with layer of small opal-A spheres and isolated patches of large opal-A spheres. (**i**) Filament covered with spheres that are *c*. 75% of filament diameter. (**j**) Filament encased by opal-A silica. (**k**) Filament covered with small opal-A spheres. (**l**) Collapsed filament covered with small opal-A spheres. (**m**–**o**) Bacteriform microbes, of various sizes, exhibiting different styles of silicification. (**p**, **q**) Rod-shaped microbes. (**r**) Silicified microbes encased, at regular intervals, with larger-diameter bands of opal-A (arrows) formed of small spheres. Regular spacing suggests that they mark locations of septa.

The distribution pattern of the opal-A spheres on some microbes suggests that their nucleation sites followed a regular pattern that was probably governed by the type and spacing of the organic ligands, which varies between different taxa. Thus, although precipitation is driven by purely physicochemical processes, some microbes may still influence the initial pattern of silica precipitation. Nevertheless, that influence can only apply to the first layer of encrusting silica. The morphology of the opal-A spheres in subsequent layers will be controlled by purely physicochemical factors, and therefore is independent of the host microbe. Smith *et al*. (2003) described a situation in highly supersaturated geothermal fluids where flocs of silica microspheres were deposited on bacterial surfaces and underwent overgrowth. However, in the examples from Iodine Pool, most nucleation appears to have taken place upon the microbial substrates, rather than by adhesion of descending suspended spheres, produced by silica polymerization in the pool. The regular distribution pattern of silica spheres on some microbe surfaces (Fig. 9b and c) cannot be explained easily by random settling.

In the case of Iodine Pool, the masking processes took place in $<$90 h. Importantly, such rapid development of the outer masking layers means that the identification of the host microbe, in terms of extant taxa, becomes even more difficult. Diagenetic processes, which begin very soon after sinter precipitation and deposition in modern hot springs (Smith *et al*. 2003), can further accelerate the loss of morphological information. After diagenesis and the conversion of the opal to quartz, much of the textural and fabric detail is destroyed (Herdianita *et al*. 2000; Guidry & Chafetz 2003), so the possibilities for accurate identification become slim.

The silicification of microbes in modern geothermal systems has received considerable attention because they may be the best analogues for understanding how ancient microbes, including those in the Precambrian, were preserved (e.g. Schultze-Lam *et al*. 1995; Konhauser & Ferris 1996; Konhauser 2000; Konhauser *et al*. 2001). It is becoming increasingly evident, however, that the preservation of the microbes in these systems is not as good as was first thought, mainly because the silicification process commonly destroys many of their taxonomically important features (e.g. Jones *et al*. 2001). In most cases, detailed information on the cellular structures of microbes preserved in ancient cherts will be apparent only if organic matter was preserved (Walter *et al*. 1998) or if the sheaths were impregnated with minerals such as iron oxide at an early stage in their taphonomic history (e.g. Ferris *et al*. 1988; Walter *et al*. 1998). The carbonaceous films that commonly outline the microbe morphology in ancient cherts are not usually preserved in sinters (e.g. Guidry & Chafetz 2003) and mineralization by minerals other than opal-A is generally rare. This study shows that replacement by opal-A, despite the fact that it is almost instantaneous on the geological time scale, may not preserve those features of the microbes that are critical to their identification in terms of extant taxa. Clearly, the analysis of ancient silicified microbes must be approached with great caution, especially if the objective is to gain insights into the nature of ancient environments based on the identification of those microbes.

## Conclusions

Glass slides were covered with collapsed unsilicified microbes, partly silicified microbes, silicified microbes and pseudofilaments within 90 h of being submerged in silica-rich waters of Iodine Pool. Description of the silicified microbes is limited to physical attributes such as filament length, filament diameter, the presence or absence of a sheath, and the presence or absence of septa (Jones *et al*. 2001). Such descriptors are generally insufficient to ally them with extant taxa that are commonly characterized on the basis of culture conditions, the presence of various soft parts in the cells, or DNA. This problem is highlighted by the fact that only two of the silicified microbes could be tentatively allied with any of the collapsed, unsilicified microbes despite the fact that they are found on the same glass slides.

The results from Iodine Pool clearly demonstrate that the identification of silicified microbes must be approached with caution, a conclusion that echoes Francis *et al*. (1978), who stated, on the basis of their experimental silicification of microbes, that: 'The fossil materials simply lack the morphological and physiological detail that must provide the basis of systematization'.

We are grateful to the Natural Sciences and Engineering Research Council of Canada, which funded this research (grants A6090 to B.J.; GP0000629 to R.W.R.; 249565-02 to K.K.); H. James, CEO of the Waimangu Volcanic Valley, who kindly gave us permission to collect samples from Iodine Pool; the New Zealand Department of Conservation, which issued the permit for collecting; and G. Braybrook (University of Alberta), who took most of the scanning electron micrographs used in this study.

## References

Awramik, S.M. 1992. The oldest records of photosynthesis. *Photosynthesis Research*, **33**, 75–89.

Bartley, J.K. 1996. Actualistic taphonomy of cyanobacteria: implications for the Precambrian fossil record. *Palaios*, **11**, 571–586.

Birnbaum, S.J., Wireman, J.W. & Borowski, R. 1989. Silica precipitation induced by the anaerobic sulfate reducing bacterium *Desulfovibrio desulfuricans*: effects upon cell morphology and implications for preservation. *In:* Crick, R.E. (ed.) *Origin, Evolution and Modern Aspects of Biomineralization in Plants and Animals*. Plenum, New York, 507–516.

Brasier, M.D., Green, O.R. & Jephcoat, A.P. *et al*. 2002. Questioning the evidence for Earth's oldest fossils. *Nature*, **416**, 76–81.

Buick, R. 1990. Microfossil recognition in Archean rocks: an appraisal of spheroids and filaments from 3500 M.Y. old chert–barite unit at North Ole, Western Australia. *Palaios*, **5**, 41–45.

Fein, J.B., Scott, S. & Rivera, N. 2002. The effect of Fe on Si adsorption by *Bacillus subtilis* cell walls: insights into the non-metabolic bacterial precipitation of silicate minerals. *Chemical Geology*, **182**, 265–273.

Ferris, F.G. 1993. Microbial biomineralization in natural environments. *Earth Science (Chikyu Kagaku)*, **47**, 233–250.

Ferris, F.G., Beveridge, T.J. & Fyfe, W.S. 1986. Iron–silica crystallite nucleation by bacteria in a geothermal sediment. *Nature*, **320**, 609–611.

Ferris, F.G., Fyfe, W.S. & Beveridge, T.J. 1988. Metallic ion binding by *Bacillus subtilis*: implications for the fossilization of microorganisms. *Geology*, **16**, 149–152.

Fortin, D. & Beveridge, T.J. 1997. Role of *Thiobacillus* in the formation of silicates in acidic mining tailings. *Chemical Geology*, **141**, 235–250.

Francis, S., Margulis, L. & Barghoorn, E.S. 1978. On the experimental silicification of microorganisms. II. On the time of appearance of eukaryotic organisms in the fossil record. *Precambrian Research*, **6**, 65–100.

Giggenbach, W.F. 1995. Variations in the chemical and isotopic composition of fluids discharged from the Taupo volcanic zone, New Zealand. *Journal of Volcanology and Geothermal Research*, **68**, 89–116.

Guidry, S.A. & Chafetz, H.S. 2003. Depositional facies and diagenetic alteration in a relict siliceous hot-spring accumulation: examples from Yellowstone National Park, U.S.A. *Journal of Sedimentary Research*, **73**, 806–823.

Herdianita, N.R., Browne, P.R.L., Rodgers, K.A. & Campbell, K.A. 2000. Mineralogical and morphological changes accompanying aging of siliceous sinter and silica residue. *Mineralium Deposita*, **35**, 48–62.

Jones, B., Renaut, R.W. & Rosen, M.R. 2001. Taphonomy of silicified filamentous microbes in modern geothermal sinters—implications for identification. *Palaios*, **16**, 580–592.

Konhauser, K.O. 2000. Hydrothermal bacterial biomineralization: potential modern-day analogues for banded iron-formations. *In:* Glenn, C.R., Prévôt-Lucas, L. & Lucas, J. (eds) *Marine Authigenesis: From Global to Microbial*. SEPM Special Publication, **66**, 133–145.

Konhauser, K.O. & Ferris, F.G. 1996. Diversity of iron and silica precipitation by microbial mats in hydrothermal waters, Iceland: implications for Precambrian iron formations. *Geology*, **24**, 323–326.

Konhauser, K.O., Fyfe, W.S., Ferris, F.G. & Beveridge, T.J. 1993. Metal sorption and mineral precipitation by bacteria in two Amazonian river systems: Rio Solimoes and Rio Negro, Brazil. *Geology*, **21**, 1103–1106.

Konhauser, K.O., Phoenix, V.R., Bottrell, S.H., Adams, D.G. & Head, I.M. 2001. Microbial–silica interactions in Icelandic hot spring sinter: possible analogues for some Precambrian siliceous stromatolites. *Sedimentology*, **48**, 415–433.

Krumbein, W.E. & Werner, D. 1983. The microbial silica cycle. *In:* Krumbein, W.E. (ed.) *Microbial Geochemistry.* Blackwell, London, 125–157.

Merz, M.U.E. 1992. The biology of carbonate precipitation by cyanobacteria. *Facies*, **26**, 81–102.

Mountain, B.W., Benning, L.G. & Boerema, J. 2002. Biomineralization in New Zealand geothermal areas; rates of growth and trace metal incorporation. *Sixth International Symposium on the Geochemistry of the Earth's Surface, Abstracts Volume*, **6**, 276–282.

Mountain, B.W., Benning, L.G. & Boerema, J. 2003. Experimental studies on New Zealand hot spring sinters: rates of growth and trace metal incorporation. *Canadian Journal of Earth Sciences*, **40**, 1643–1667.

Oehler, J.H. 1976. Experimental studies in Precambrian paleontology: structural and chemical changes in blue–green algae during simulated fossilization in synthetic chert. *Geological Society of America Bulletin*, **87**, 117–129.

Oehler, L.H. & Schopf, J.W. 1971. Artificial microfossils: experimental studies of permineralization of blue–green algae in silica. *Science*, **174**, 1229–1231.

Phoenix, V.R., Konhauser, K.O. & Ferris, F.G. 2003. Experimental study of iron and silica immobilization by bacteria in mixed Fe–Si systems: implications for microbial silicification in host springs. *Canadian Journal of Earth Sciences*, **40**, 1669–1678.

Rasmussen, B. 2000. Filamentous microfossils in a 3,235-million-year-old volcanogenic massive sulphide deposit. *Nature*, **405**, 676–679.

Riding, R. 1991. Classification of microbial carbonates. *In:* Riding, R. (ed.) *Calcareous Algae and Stromatolites*. Springer, Berlin, 21–51.

Rosing, M.T. 1999. $^{13}$C-depleted carbon microparticles in >3700-Ma sea-floor sedimentary rocks from Greenland. *Science*, **283**, 674–676.

Schopf, J.W. 1993. Microfossils of the early Archean Apex Chert: new evidence of the antiquity of life. *Science*, **260**, 640–645.

Schopf, J.W. 1994. The oldest record of life: Early Archean stromatolites, microfossils, and organic matter. *In:* Bengtson, S. (ed.) *Early Life on Earth*. Columbia University Press, New York, 270–286.

Schopf, J.W. & Packer, B.M. 1987. Early Archean (3.3-billion to 3.5-billion-year-old) microfossils from Warrawoona Group, Australia. *Science*, **237**, 70–72.

Schopf, J.W., Kudryavtsev, A.B., Agresti, D.G., Wdowiak, T.J. & Czaja, A.D. 2002. Laser–Raman imagery of Earth's earliest fossils. *Nature*, **416**, 73–76.

Schultze-Lam, S., Thompson, J. & Beveridge, T.J. 1993. Metal ion immobilization by bacterial surfaces in freshwater environments. *Water Pollution Research Journal of Canada*, **28**, 51–81.

Schultze-Lam, S., Ferris, F.G., Konhauser, K.O. & Wiese, R.G. 1995. In situ silicification of an Icelandic hot spring microbial mat: implications for microfossil formation. *Canadian Journal of Earth Sciences*, **32**, 2021–2026.

Scott, B. 1992. *Waimangu: a volcanic encounter*. Waimangu Volcanic Valley, Rotorua, New Zealand.

Seward, T.M. & Sheppard, D.S. 1986. Waimangu geothermal field. *In:* Henley, J.W., Hedenquist, J.W. & Roberts, P.J. (eds) *Guide to the Active Epithermal (Geothermal) Systems and Precious Metal Deposits of New Zealand*. Monograph Series on Mineral Deposits, **26**, 81–91.

Shen, Y., Buick, R. & Canfield, D.E. 2001. Isotopic evidence for microbial sulphate reduction in the early Archean era. *Nature*, **410**, 77–81.

Sheppard, D.S. 1986. Fluid chemistry of the Waimangu geothermal system. *Geothermics*, **15**, 309–328.

Simmons, S.F., Stewart, M.K., Robinson, B.W. & Glover, R.B. 1994. The chemical and isotopic compositions of thermal waters at Waimangu, New Zealand. *Geothermics*, **23**, 539–553.

Smith, B.Y., Turner, S.J. & Rodgers, K.A. 2003. Opal-A and associated microbes from Wairakei, New Zealand: the first 300 days. *Mineralogical Magazine*, **67**, 563–579.

Toporski, J.K.W., Steele, A., Westall, F., Thomas-Keprta, K.L. & McKay, D.S. 2002. The simulated silicification of bacteria—new clues to the modes and timing of bacterial preservation and implications for the search for extraterrestrial microfossils. *Astrobiology*, **2**, 1–26.

Walsh, M.M. 1992. Microfossils and possible microfossils from the Early Archean Onverwacht Group, Barberton Mountain Land, South Africa. *Precambrian Research*, **54**, 271–293.

Walsh, M.M. & Lowe, D.R. 1985. Filamentous microfossils from 3,500-Myr-old Onverwacht Group, Barberton Mountain Land, South Africa. *Nature*, **314**, 530–532.

Walter, M.R. 1976. Geyserites in Yellowstone National Park: an example of abiogenic 'stromatolites'. *In:* Walter, M.R. (ed.) *Stromatolites*. Developments in Sedimentology, **20**, 87–112.

Walter, M.R., McLoughlin, S., Drinnan, A.N. & Farmer, J.D. 1998. Palaeontology of Devonian thermal spring deposits, Drummond Basin, Australia. *Alcheringa*, **22**, 285–314.

Westall, F. 1997. The influence of cell wall composition on the fossilization of bacteria and the implications for the search for early life forms. *In:* Cosmovici, S., Bowyer, S. & Werthimer, D. (eds) *Astronomical and Biochemical Origins and the Search for Life in the Universe*. Editori Compositrici, Bologna, 491–504.

Westall, F., Boni, L. & Guerzoni, E. 1995. The experimental silicification of microorganisms. *Palaeontology*, **38**, 495–528.

Westall, F., de Wit, M.J., Dann, J., van der Gaast, S., de Ronde, C.E.J. & Gerneke, D. 2001. Early Archean fossil bacteria and biofilms in hydrothermally-influenced sediments from the Barberton greenstone belt, South Africa. *Precambrian Research*, **106**, 93–116.

White, D.E., Brannock, W.W. & Murata, K.J. 1956. Silica in hot-spring waters. *Geochimica et Cosmochimica Acta*, **10**, 27–59.

Yee, N., Phoenix, V.R., Konhauser, K.O., Benning, L.G. & Ferris, F.G. 2003. The effect of cyanobacteria on silica precipitation at neutral pH: implications for bacterial silicification in geothermal hot springs. *Chemical Geology*, **199**, 83–90.

Received 11 November 2003; revised typescript accepted 16 May 2004.
Scientific editing by Alistair Crame